Polarized nucleon structure functions within a chiral soliton model

H. Weigel, L. Gamberg,* and H. Reinhardt
Institute for Theoretical Physics, Tübingen University, Auf der Morgenstelle 14, D-72076 Tübingen, Germany
(Received 3 September 1996; revised manuscript received 17 January 1997)

We study polarized-spin structure functions of the nucleon within the bosonized Nambu–Jona-Lasinio model where the nucleon emerges as a chiral soliton. We present the electromagnetic polarized structure functions $g_1(x)$ and $g_2(x)$ for ep scattering and discuss various sum rules in the valence quark approximation. This approximation is justified because in this model axial properties of the nucleon are dominated by their valence quark contributions. We find that these structure functions are well localized in the interval $0 \leqslant x \leqslant 1$. We compare the model predictions on the polarized structure functions with data from the E143 experiment by evolving them from the scale characteristic of the NJL model to the scale of the data. Additionally, a comparison is made with parametrized data at a momentum scale commensurate with the model calculation. [S0556-2821(97)05611-7]

PACS number(s): 12.39.Fe, 12.39.Ki

I. INTRODUCTION

Over the past decade, beginning with the measurement of nucleon spin–polarized structure function $g_1(x,Q^2)$ by the European Muon Collaboration (EMC) [1] at CERN and most recently with the spin-structure function $g_2(x,Q^2)$ in the E143 experiment [2] at SLAC, a wealth of information has been gathered on the spin–polarized structure functions of the nucleon and their corresponding sum rules (see, in addition, [3–8]). Initially, the analysis of these experiments cast doubt on the nonrelativistic quark model [9] interpretations regarding the spin content of the proton. By now, it is firmly established that the quark helicity of the nucleon is much smaller than the predictions of that model, however, many questions remain to be addressed concerning the spin structure. As a result there have been numerous investigations within models for the nucleon in an effort to determine the manner in which the nucleon spin is distributed among its constituents. One option is to study the axial-vector current matrix elements of the nucleon such as $\langle N|\mathcal{A}^i_\mu|N\rangle = 2\Delta q_i S_\mu$, which, for example, provide information on the nucleon axial singlet charge

$$g_A^0 = \langle N|\mathcal{A}_3^0|N\rangle = (\Delta u + \Delta d + \Delta s) = \Gamma_1^p(Q^2) + \Gamma_1^n(Q^2). \tag{1}$$

Here Δq are the axial charges of the quark constituents and $\Gamma_1^N(Q^2) = \int_0^1 dx g_1^N(x,Q^2)$ is the first moment of the longitudinal nucleon spin-structure function $g_1^N(x,Q^2)$. Of course, it is more illuminating to directly compute the longitudinal and transverse nucleon spin-structure functions, $g_1(x,Q^2)$ and $g_T(x,Q^2) = g_1(x,Q^2) + g_2(x,Q^2)$, respectively, as functions of the Bjorken variable x. We will calculate these structure functions within the Nambu–Jona-Lasinio (NJL) [10] chiral soliton model [11].

Chiral soliton models are unique both in being the first effective models of hadronic physics to shed light on the so-called ''proton-spin crisis'' by predicting a singlet combination in accord with the data [12], and in predicting a nontrivial strange quark content to the axial-vector current of the nucleon [12–15]; about 10–30 % of the down quarks (see [16,17] for reviews). However, while the leading moments of these structure functions have been calculated within chiral soliton models, from the Skyrme model [18,19] and its various vector-meson extensions, to models containing explicit quark degrees of freedom such as the (NJL) model [10], the nucleon spin-structure functions themselves have not been investigated in these models. Soliton model calculations of structure functions were, however, performed in Friedberg-Lee [20] and color-dielectric [21] models. In addition, structure functions have extensively been studied within the framework of effective quark models such as the bag model [22], and the center-of-mass bag model [23]. These models are confining by construction but they neither contain nonperturbative pseudoscalar fields nor are they chirally symmetric.[1] To this date it is fair to say that many of the successes of low–energy effective models rely on the incorporation of chiral symmetry and its spontaneous symmetry breaking (see, e.g., [26]). In this article we, therefore, present our calculation of the polarized-spin structure functions in the NJL chiral soliton model [27,26]. Since in particular, the static axial properties of the nucleon are dominated by the valence quark contribution in this model it is legitimate to focus on the valence quarks in this model.

At the outset it is important to note that a major difference between the chiral soliton models and models previously employed to calculate structure functions is the form of the nucleon wave function. In the latter the nucleon wave function is a product of Dirac spinors while in the former the nucleon appears as a collectively excited (topologically) nontrivial meson configuration.

As in the original bag model study [28] of structure functions for localized field configurations, the structure functions are most easily accessible when the current operator is

*Present address: Department of Physics and Astronomy, University of Oklahoma, 440 West Brooks, Norman, OK 73019.

[1] In the cloudy bag model the contribution of the pions to structure functions has at most been treated perturbatively [24,25].

at most quadratic in the fundamental fields and the propagation of the interpolating field can be regarded as free. Although the latter approximation is well justified in the Bjorken limit the former condition is difficult to satisfy in soliton models where mesons are fundamental fields (e.g., the Skyrme model [18,19], the chiral quark model of Ref. [29], or the chiral bag model [30]). Such model Lagrangians typically possess all orders of the fundamental pion field. In that case the current operator is not confined to quadratic order and the calculation of the hadronic tensor [see Eq. (2) below] requires drastic approximations. In this respect the chirally invariant NJL model is preferred because it is entirely defined in terms of quark degrees of freedom and formally the current possesses the structure as in a noninteracting model. This makes the evaluation of the hadronic tensor feasible. Nevertheless, after bosonization the hadronic currents are uniquely defined functionals of the solitonic meson fields.

The paper is organized as follows: In Sec. II we give a brief discussion of the standard operator product expansion (OPE) analysis to establish the connection between the effective models for the baryons at low energies and the quark-parton model description. In Sec. III we briefly review the NJL chiral soliton. In Sec. IV we extract the polarized structure functions from the hadronic tensor, Eq. (16) exploiting the ''valence quark approximation.'' Section V displays the results of the spin-polarized structure functions calculated in the NJL chiral soliton model within this approximation and compare this result with a recent low-renormalization point parametrization [31]. In Sec. VI we use Jaffe's prescription [32] to impose proper support for the structure function within the interval $x\in[0,1]$. Subsequently, the structure functions are evolved [33–35] from the scale characterizing the NJL model to the scale associated with the experimental data. Section VII serves to summarize these studies and to propose further explorations. In Appendix A we list explicit analytic expressions for the isoscalar and isovector polarized structure functions. Appendix B summarizes details on the evolution of the twist-three structure function $\overline{g}_2(x,Q^2)$.

II. DIS AND THE CHIRAL SOLITON

It has been a long-standing effort to establish the connection between the chiral soliton picture of the baryon, which essentially views baryons as mesonic lumps and the quark-parton model which regards baryons as composites of almost noninteracting, pointlike quarks. While the former has been quite successful in describing static properties of the nucleon, the latter, being firmly established within the context of deep-inelastic scattering (DIS), has been employed extensively to calculate the short-distance or perturbative processes within QCD. In fact, this connection can be made through the OPE.

The discussion begins with the hadronic tensor for electron-nucleon scattering:

$$W_{\mu\nu}(q)=\frac{1}{4\pi}\int d^4\xi e^{iq\cdot\xi}\langle N|[J_\mu(\xi),J_\nu^\dagger(0)]|N\rangle, \qquad (2)$$

where $J_\mu=\overline{q}(\xi)\gamma_\mu\mathcal{Q}q(\xi)$ is the electromagnetic current, $\mathcal{Q}=(\frac{2}{3},-\frac{1}{3})$ is the (two-flavor) quark charge matrix, and $|N\rangle$ refers to the nucleon state. In the DIS regime the OPE enables one to express the product of these currents in terms of the forward Compton scattering amplitude $T_{\mu\nu}(q)$ of a virtual photon from a nucleon

$$T_{\mu\nu}(q)=i\int d^4\xi e^{iq\cdot\xi}\langle N|T(J_\mu(\xi)J_\nu^\dagger(0))|N\rangle, \qquad (3)$$

by an expansion on the light cone ($\xi^2\to 0$) using a set of renormalized local operators [36–38]. In the Bjorken limit the influence of these operators is determined by the twist τ or the light-cone singularity of their coefficient functions. Effectively, this becomes a power series in the inverse of the Bjorken variable $x=-q^2/2P\cdot q$, with P_μ being the nucleon momentum:

$$T_{\mu\nu}(q)=\sum_{n,i,\tau}\left(\frac{1}{x}\right)^n e^i_{\mu\nu}(q,P,S) \times C^n_{\tau,i}(Q^2/\mu^2,\alpha_s(\mu^2))O^n_{\tau,i}(\mu^2)\left(\frac{1}{Q^2}\right)^{\tau/2-1}. \qquad (4)$$

Here the index i runs over all scalar matrix elements $O^n_{\tau,i}(\mu^2)$, with the same Lorentz structure (characterized by the tensor $e^i_{\mu\nu}$). Furthermore, S^μ is the spin of the nucleon ($S^2=-1, S\cdot P=0$) and $Q^2=-q^2>0$. As is evident, higher twist contributions are suppressed by powers of $1/Q^2$. The coefficient functions $C^n_{\tau,i}(Q^2/\mu^2,\alpha_s(\mu^2))$ are target independent and in principle include all QCD radiative corrections. Their Q^2 variation is determined from the solution of the renormalization group equations and varies logarithmically at large Q^2. On the other hand, the reduced matrix elements $O^n_{\tau,i}(\mu^2)$ depend only on the renormalization scale μ^2 and reflect the nonperturbative properties of the nucleon [39].

The optical theorem states that the hadronic tensor is given in terms of the imaginary part of the virtual Compton scattering amplitude, $W_{\mu\nu}=(1/2\pi)\mathrm{Im}T_{\mu\nu}$. From the analytic properties of $T_{\mu\nu}(q)$, together with Eq. (4), an infinite set of sum rules results for the form factors $\mathcal{W}_i(x,Q^2)$, which are defined via the Lorentz-covariant decomposition $W_{\mu\nu}(q)=e^i_{\mu\nu}\mathcal{W}_i(x,Q^2)$. These sum rules read

$$\int_0^1 dx x^{n-1}\mathcal{W}_i(y,Q^2)=\sum_\tau C^n_{\tau,i}(Q^2/\mu^2,\alpha_s(\mu^2))O^n_{\tau,i}(\mu^2) \times\left(\frac{1}{Q^2}\right)^{\tau/2-1}. \qquad (5)$$

In the *impulse approximation* (i.e., neglecting radiative corrections) [36,40,41], one can directly sum the OPE gaining direct access to the structure functions in terms of the reduced matrix elements $O^n_{\tau,i}(\mu^2)$.

When calculating the renormalization scale-dependent matrix elements $O^n_{\tau,i}(\mu^2)$ within QCD, μ^2 is an arbitrary parameter adjusted to ensure rapid convergence of the perturbation series. However, given the difficulties of obtaining a satisfactory description of the nucleon as a bound state in the Q^2 regime of DIS processes it is customary to calculate these matrix elements in models at a low scale μ^2 and sub-

sequently evolve these results to the relevant DIS momentum region of the data employing, for example, the Altarelli-Parisi evolution [33,34]. In this context, the scale $\mu^2 \sim \Lambda^2_{\rm QCD}$ characterizes the nonperturbative regime where it is possible to formulate a nucleon wave function from which structure functions are computed.

Here we will utilize the NJL chiral soliton model to calculate the spin-polarized nucleon structure functions at the scale μ^2, subsequently evolving the structure functions according to the Altarelli–Parisi scheme. This establishes the connection between chiral soliton and the parton models. In addition, we compare the structure functions calculated in the NJL model to a parametrization of spin structure function [31] at a scale commensurate with our model.

III. THE NUCLEON STATE IN THE NJL MODEL

The Lagrangian of the NJL model reads

$$\mathcal{L} = \overline{q}(i\partial\!\!\!/ - m^0)q + 2G_{\rm NJL}\sum_{i=0}^{3}\left[\left(\overline{q}\frac{\tau^i}{2}q\right)^2 + \left(\overline{q}\frac{\tau^i}{2}i\gamma_5 q\right)^2\right]. \tag{6}$$

Here $q, \hat{m}^0$, and $G_{\rm NJL}$ denote the quark field, the current quark mass, and a dimensionful coupling constant, respectively. When integrating out the gluon fields from QCD a current-current interaction remains, which is meditated by the gluon propagator. Replacing this gluon propagator by a local contact interaction and performing the appropriate Fierz transformations yields the Lagrangian (6) in leading order of $1/N_c$ [42], where N_c refers to the number of color degrees of freedom. It is hence apparent that the interaction term in Eq. (6) is a remnant of the gluon fields. Hence, gluonic effects are included in the model described by the Lagrangian (6).

Application of functional bosonization techniques [43] to the Lagrangian (6) yields the mesonic action

$$\mathcal{A} = {\rm Tr}_\Lambda \ln(iD) + \frac{1}{4G_{\rm NJL}}\int d^4x\, {\rm tr}[m^0(M+M^\dagger) - MM^\dagger], \tag{7}$$

$$D = i\partial\!\!\!/ - (M+M^\dagger) - \gamma_5(M-M^\dagger). \tag{8}$$

The composite scalar (S) and pseudoscalar (P) meson fields are contained in $M=S+iP$ and appear as quark-antiquark bound states. The NJL model embodies the approximate chiral symmetry of QCD and has to be understood as an effective (nonrenormalizable) theory of the low-energy quark flavor dynamics. For regularization, which is indicated by the cutoff Λ, we will adopt the proper-time scheme [44]. The free parameters of the model are the current quark mass m^0, the coupling constant $G_{\rm NJL}$, and the cutoff Λ. Upon expanding $\mathcal{A}$ to quadratic order in M these parameters are related to the pion mass $m_\pi = 135$ MeV and pion decay constant $f_\pi = 93$ MeV. This leaves one undetermined parameter which we choose to be the vacuum expectation value $m = \langle M \rangle$. For apparent reasons m is called the constituent quark mass. It is related to $m^0, G_{\rm NJL}$, and Λ via the gap equation, i.e., the equation of motion for the scalar field S [43]. The occurrence of this vacuum expectation value reflects the spontaneous breaking of chiral symmetry and causes the pseudoscalar fields to emerge as (would-be) Goldstone bosons.

As the NJL model soliton has exhaustively been discussed in recent review articles [26,45], we only present those features which are relevant for the computation of the structure functions in the valence quark approximation.

The chiral soliton is given by the hedgehog configuration of the meson fields

$$M_{\rm H}(\boldsymbol{x}) = m\exp[i\boldsymbol{\tau}\cdot\boldsymbol{x}\Theta(r)]. \tag{9}$$

In order to compute the functional trace in Eq. (7) for this static configuration we express the Dirac operator (8) as $D = i\gamma_0(\partial_t - h)$, where

$$h = \boldsymbol{\alpha}\cdot\boldsymbol{p} + m\exp[i\gamma_5\boldsymbol{\tau}\cdot\hat{\boldsymbol{x}}\Theta(r)] \tag{10}$$

is the corresponding Dirac Hamiltonian. We denote the eigenvalues and eigenfunctions of h by ϵ_μ and $\Psi_\mu(\mathbf{x})$, respectively. Explicit expressions for these wave functions are displayed in Appendix A. In the proper-time regularization scheme the energy functional of the NJL model is found to be [27,26]

$$E[\Theta] = \frac{N_C}{2}\epsilon_v[1+{\rm sgn}(\epsilon_v)] + \frac{N_C}{2}\int_{1/\Lambda^2}^{\infty}\frac{ds}{\sqrt{4\pi s^3}} \times \sum_\nu \exp(-s\epsilon_\nu^2) + m_\pi^2 f_\pi^2 \int d^3r[1-\cos\Theta(r)], \tag{11}$$

with $N_C = 3$ being the number of color degrees of freedom. The subscript ''v'' denotes the valence quark level. This state is the distinct level bound in the soliton background, i.e., $-m < \epsilon_v < m$. The chiral angle $\Theta(r)$ is obtained by self-consistently extremizing $E[\Theta]$ [11].

States possessing good spin and isospin quantum numbers are generated by rotating the hedgehog field [19]:

$$M(\boldsymbol{x},t) = A(t)M_{\rm H}(\boldsymbol{x})A^\dagger(t), \tag{12}$$

which introduces the collective coordinates $A(t) \in {\rm SU}(2)$. The action functional is expanded [27] in the angular velocities

$$2A^\dagger(t)\dot{A}(t) = i\boldsymbol{\tau}\cdot\boldsymbol{\Omega}. \tag{13}$$

In particular, the valence quark wave function receives a first-order perturbation

$$\Psi_v(\boldsymbol{x},t) = e^{-i\epsilon_v t}A(t)\left\{\Psi_v(\boldsymbol{x}) + \frac{1}{2}\sum_{\mu\neq v}\Psi_\mu(\boldsymbol{x})\frac{\langle\mu|\boldsymbol{\tau}\cdot\boldsymbol{\Omega}|v\rangle}{\epsilon_v - \epsilon_\mu}\right\} =: e^{-i\epsilon_v t}A(t)\psi_v(\boldsymbol{x}). \tag{14}$$

Here $\psi_v(\boldsymbol{x})$ refers to the spatial part of the body-fixed valence quark wave function with the rotational corrections included. Nucleon states $|N\rangle$ are obtained by canonical quantization of the collective coordinates $A(t)$. By construction these states live in the Hilbert space of a rigid rotator. The eigenfunctions are Wigner D functions

$$\langle A|N\rangle = \frac{1}{2\pi} D^{1/2}_{I_3,-J_3}(A), \tag{15}$$

with I_3 and J_3 being, respectively, the isospin and spin projection quantum numbers of the nucleon.

IV. POLARIZED STRUCTURE FUNCTIONS IN THE NJL MODEL

The starting point for computing nucleon structure functions is the hadronic tensor, Eq. (2). The polarized structure functions are extracted from its antisymmetric piece, $W^{(A)}_{\mu\nu} = (W_{\mu\nu} - W_{\nu\mu})/2i$. Lorentz invariance implies that the antisymmetric portion, characterizing polarized lepton-nucleon scattering, can be decomposed into the polarized structure functions, $g_1(x,Q^2)$ and $g_2(x,Q^2)$:

$$W^{(A)}_{\mu\nu}(q) = i\epsilon_{\mu\nu\lambda\sigma}\frac{q^\lambda M_N}{P\cdot q}\left\{ g_1(x,Q^2)S^\sigma + \left(S^\sigma - \frac{q\cdot S}{q\cdot p}P^\sigma\right) g_2(x,Q^2)\right\}, \tag{16}$$

again, P_μ refers to the nucleon momentum and $Q^2 = -q^2$. The tensors multiplying the structure functions in Eq. (16) should be identified with the Lorentz tensors $e^i_{\mu\nu}$ in Eq. (4).

Contracting $W^{(A)}_{\mu\nu}$ with the longitudinal $\Lambda^{\mu\nu}_L$ and transverse $\Lambda^{\mu\nu}_T$ projection operators [39],

$$\Lambda^{\mu\nu}_L = \frac{2}{b}\left\{ 2P\cdot qxS_\lambda + \frac{1}{q\cdot S}\left[(q\cdot S)^2 - \left(\frac{P\cdot q}{M}\right)^2\right] q_\lambda\right\} P_\tau \epsilon^{\mu\nu\lambda\tau}, \tag{17}$$

$$\Lambda^{\mu\nu}_T = \frac{2}{b}\left\{ \left[\left(\frac{P\cdot q}{M}\right)^2 + 2P\cdot qx\right] S_\lambda + (q\cdot S)q_\lambda\right\} P_\tau \epsilon^{\mu\nu\lambda\tau}, \tag{18}$$

and choosing the pertinent polarization, yields the longitudinal component

$$g_L(x,Q^2) = g_1(x,Q^2), \tag{19}$$

as well as the transverse combination

$$g_T(x,Q^2) = g_1(x,Q^2) + g_2(x,Q^2). \tag{20}$$

Also, $b = -4M\{(P\cdot q/M)^2 + 2P\cdot qx - (q\cdot S)^2\}$. In the Bjorken limit, which corresponds to the kinematical regime

$$q_0 = |\boldsymbol{q}| - M_N x \quad \text{with} \quad |\boldsymbol{q}| \to \infty, \tag{21}$$

the antisymmetric component of the hadronic tensor becomes [28]

$$W^{(A)}_{\mu\nu}(q) = \int \frac{d^4k}{(2\pi)^4}\epsilon_{\mu\rho\nu\sigma}k^\rho \mathrm{sgn}(k_0)\,\delta(k^2)\int_{-\infty}^{+\infty} dt e^{i(k_0+q_0)t} \times \int d^3x_1 \int d^3x_2 \exp[-i(\boldsymbol{k}+\boldsymbol{q})\cdot(\boldsymbol{x}_1-\boldsymbol{x}_2)] \times \langle N|\{\overline{\Psi}(\boldsymbol{x}_1,t)\mathcal{Q}^2\gamma^\sigma\gamma^5\Psi(\boldsymbol{x}_2,0) + \overline{\Psi}(\boldsymbol{x}_2,0)\mathcal{Q}^2\gamma^\sigma\gamma^5\Psi(\boldsymbol{x}_1,t)\}|N\rangle, \tag{22}$$

where $\epsilon_{\mu\rho\nu\sigma}\gamma^\sigma\gamma^5$ is the antisymmetric combination of $\gamma_\mu\gamma_\rho\gamma_\nu$. The matrix element between the nucleon states is to be taken in the space of the collective coordinates $A(t)$ [see Eqs. (12) and (15)] as the object in curly brackets is an operator in this space. In deriving the expression (22) the *free* correlation function for the intermediate quark fields has been assumed[2] after applying Wick's theorem to the product of quark currents in Eq. (2) [28]. The use of the *free* correlation function is justified because in the Bjorken limit (21), the intermediate quark fields carry very large momenta and are hence not sensitive to typical soliton momenta. This procedure reduces the commutator $[J_\mu(\boldsymbol{x}_1,t), J^\dagger_\nu(\boldsymbol{x}_2,0)]$ of the quark currents in the definition (2) to objects which are merely bilinear in the quark fields. Consequently, in the Bjorken limit (21) the momentum k of the intermediate quark state is highly off shell and hence is not sensitive to momenta typical for the soliton configuration. Therefore, the use of the free correlation function is a good approximation in this kinematical regime. Accordingly, the intermediate quark states are taken to be massless, cf. Eq. (22).

Since the NJL model is originally defined in terms of quark degrees of freedom, quark bilinears as in Eq. (22) can be computed from the functional

$$\langle \overline{q}(x)\mathcal{Q}^2 q(y)\rangle = \int D\overline{q}Dq\,\overline{q}(x)\mathcal{Q}^2 q(y)\exp\left(i\int d^4x'\mathcal{L}\right) = \frac{\delta}{i\delta\alpha(x,y)}\int D\overline{q}Dq \times \exp\left(i\int d^4x' d^4y'[\delta^4(x'-y')\mathcal{L} + \alpha(x',y')\overline{q}(x')\mathcal{Q}^2 q(y')]\right)\Big|_{\alpha(x,y)=0}. \tag{23}$$

The introduction of the bilocal source $\alpha(x,y)$ facilitates the functional bosonization after which Eq. (23) takes the form

$$\frac{\delta}{\delta\alpha(x,y)}\mathrm{Tr}_\Lambda \ln[\delta^4(x-y)D + \alpha(x,y)\mathcal{Q}^2)]\big|_{\alpha(x,y)=0}. \tag{24}$$

The operator D is defined in Eq. (8). The correlation $\langle\overline{q}(x)\mathcal{Q}^2 q(y)\rangle$ depends on the angle between $\boldsymbol{x}$ and $\boldsymbol{y}$. Since in general the functional (23) involves quark states of all

[2]Adopting a dressed correlation will cause corrections starting at order twist-four in QCD [46].

angular momenta (l), a technical difficulty arises because this angular dependence has to be treated numerically. The major purpose of the present paper is to demonstrate that polarized structure functions can indeed be computed from a chiral soliton. With this in mind we will adopt the valence quark approximation where the quark configurations in Eq. (23) are restricted to the valence quark level. Accordingly, the valence quark wave function (14) is substituted into Eq. (22). Then, only quark orbital angular momenta up to $l=2$ are relevant. From a physical point of view this approximation is justified for moderate constituent quark masses ($m\approx 400$ MeV) because in that parameter region the soliton properties are dominated by their valence quark contributions [26,45]. In particular, this is the case for the axial properties of the nucleon.

In the next step the polarized structure functions, $g_1(x,\mu^2)$ and $g_T(x,\mu^2)$, are extracted according to Eqs. (17) and (18). In the remainder of this section we will omit explicit reference to the scale μ^2. We choose the frame such that the nucleon is polarized along the positive-$\mathbf{z}$ and positive-$\boldsymbol{x}$ directions in the longitudinal and transverse cases, respectively. Note also that this implies the choice $\boldsymbol{q}=q\hat{\mathbf{z}}$. When extracting the structure functions the integrations over the time coordinate in Eq. (22) can readily be done yielding the conservation of energy for forward and backward moving intermediate quarks. Carrying out the integrations over k_0 and $k=|\boldsymbol{k}|$ gives for the structure functions,

$$g_1(x)=-N_C\frac{M_N}{\pi}\Big\langle N,\frac{1}{2}\hat{\mathbf{z}}\Big|\int d\Omega_{\boldsymbol{k}}k^2\{\widetilde{\psi}_v^\dagger(\boldsymbol{p})(1-\boldsymbol{\alpha}\cdot\hat{\boldsymbol{k}})\times\gamma^5\Gamma\widetilde{\psi}_v(\boldsymbol{p})|_{k=q_0+\epsilon_v}+\widetilde{\psi}_v^\dagger(-\boldsymbol{p})(1-\boldsymbol{\alpha}\cdot\hat{\boldsymbol{k}})\times\gamma^5\Gamma\widetilde{\psi}_v(-\boldsymbol{p})|_{k=q_0-\epsilon_v}\}\Big|N,\frac{1}{2}\hat{\mathbf{z}}\Big\rangle, \tag{25}$$

$$g_T(x)=g_1(x)+g_2(x)=-N_C\frac{M_N}{\pi}\Big\langle N,\frac{1}{2}\hat{\mathbf{x}}\Big|\int d\Omega_{\boldsymbol{k}}k^2\times\{\widetilde{\psi}_v^\dagger(\boldsymbol{p})(\boldsymbol{\alpha}\cdot\hat{\boldsymbol{k}})\gamma^5\Gamma\widetilde{\psi}_v(\boldsymbol{p})|_{k=q_0+\epsilon_v}+\widetilde{\psi}_v^\dagger(-\boldsymbol{p})(\boldsymbol{\alpha}\cdot\hat{\boldsymbol{k}})\gamma^5\Gamma\widetilde{\psi}_v(-\boldsymbol{p})|_{k=q_0-\epsilon_v}\}\Big|N,\frac{1}{2}\hat{\mathbf{x}}\Big\rangle, \tag{26}$$

where $\boldsymbol{p}=\boldsymbol{k}+\boldsymbol{q}$ and $\Gamma=\frac{5}{18}\mathbb{1}+\frac{1}{6}D_{3i}\tau_i$ with $D_{ij}=\frac{1}{2}\mathrm{tr}[\tau_i A(t)\tau_j A^\dagger]$ being the adjoint representation of the collective rotation, cf. Eq. (12). The second entry in the states labels the spin orientation. N_C appears as a multiplicative factor because the functional trace (24) includes the color trace as well. Furthermore, the Fourier transform of the valence quark wave function

$$\widetilde{\psi}_v(\boldsymbol{p})=\int\frac{d^3x}{4\pi}\psi_v(\boldsymbol{x})\exp(i\boldsymbol{p}\cdot\boldsymbol{x}) \tag{27}$$

has been introduced. Also, note that the wave function ψ_v contains an implicit dependence on the collective coordinates through the angular velocity $\boldsymbol{\Omega}$, cf. Eq. (14).

The dependence of the wave function $\widetilde{\psi}_v(\pm\boldsymbol{p})$ on the integration variable $\hat{\boldsymbol{k}}$ is only implicit. In the Bjorken limit the integration variables may then be changed to [28]

$$k^2d\Omega_{\boldsymbol{k}}=pdpd\Phi,\quad p=|\boldsymbol{p}|, \tag{28}$$

where Φ denotes the azimuth angle between $\boldsymbol{q}$ and $\boldsymbol{p}$. The lower bound for the p integral is adopted when $\boldsymbol{k}$ and $\boldsymbol{q}$ are antiparallel; $p_\pm^{\min}=|M_Nx\mp\epsilon_v|$ for $k=-(q_0\pm\epsilon_v)$, respectively. Since the wave function $\widetilde{\psi}(\pm\boldsymbol{p})$ acquires its dominant support for $p\leqslant M_N$ the integrand is different from zero only when $\boldsymbol{q}$ and $\boldsymbol{k}$ are antiparallel. We may, therefore, take $\hat{\boldsymbol{k}}=-\hat{\mathbf{z}}$. This is nothing but the light-cone description for computing structure functions [41]. Although expected, this result is nontrivial and will only come out in models which have a current operator which, as in QCD, is formally identical to the one of noninteracting quarks. The valence quark state possesses positive parity yielding $\widetilde{\psi}(-\boldsymbol{p})=\gamma_0\widetilde{\psi}(\boldsymbol{p})$. With this we arrive at the expression for the isoscalar and isovector parts of the polarized structure function in the valence quark approximation:

$$g_{1,\pm}^{I=0}(x)=-N_C\frac{5M_N}{18\pi}\Big\langle N,\frac{1}{2}\hat{\mathbf{z}}\Big|\int_{M_N|x_\mp|}^\infty pdp\int_0^{2\pi}d\Phi\,\widetilde{\psi}_v^\dagger(\boldsymbol{p}_\mp)\times(1\pm\alpha_3)\gamma^5\widetilde{\psi}_v(\boldsymbol{p}_\mp)\Big|N,\frac{1}{2}\hat{\mathbf{z}}\Big\rangle, \tag{29}$$

$$g_{1,\pm}^{I=1}(x)=-N_C\frac{M_N}{6\pi}\Big\langle N,\frac{1}{2}\hat{\mathbf{z}}\Big|D_{3i}\int_{M_N|x_\mp|}^\infty pdp\int_0^{2\pi}d\Phi\,\widetilde{\psi}_v^\dagger(\boldsymbol{p}_\mp)\times\tau_i(1\pm\alpha_3)\gamma^5\widetilde{\psi}_v(\boldsymbol{p}_\mp)\Big|N,\frac{1}{2}\hat{\mathbf{z}}\Big\rangle, \tag{30}$$

$$g_{T,\pm}^{I=0}(x)=-N_C\frac{5M_N}{18\pi}\Big\langle N,\frac{1}{2}\hat{\mathbf{x}}\Big|\int_{M_N|x_\mp|}^\infty pdp\int_0^{2\pi}d\Phi\,\widetilde{\psi}_v^\dagger(\boldsymbol{p}_\mp)\times\alpha_3\gamma^5\widetilde{\psi}_v(\boldsymbol{p}_\mp)\Big|N,\frac{1}{2}\hat{\mathbf{x}}\Big\rangle, \tag{31}$$

$$g_{T,\pm}^{I=1}(x)=-N_C\frac{M_N}{6\pi}\Big\langle N,\frac{1}{2}\hat{\mathbf{x}}\Big|D_{3i}\int_{M_N|x_\mp|}^\infty pdp\int_0^{2\pi}d\Phi\times\widetilde{\psi}_v^\dagger(\boldsymbol{p}_\mp)\tau_i\alpha_3\gamma^5\widetilde{\psi}_v(\boldsymbol{p}_\mp)\Big|N,\frac{1}{2}\hat{\mathbf{x}}\Big\rangle, \tag{32}$$

where $x_\pm=x\pm\epsilon_v/M_N$ and $\cos(\Theta_p^\pm)=M_Nx_\pm/p$. The complete structure functions are given by

$$g_1(x)=g_{1,+}^{I=0}(x)+g_{1,+}^{I=1}(x)-(g_{1,-}^{I=0}(x)-g_{1,-}^{I=1}(x)) \tag{33}$$

$$g_T(x)=g_{T,+}^{I=0}(x)+g_{T,+}^{I=1}(x)-(g_{T,-}^{I=0}(x)-g_{T,-}^{I=1}(x)). \tag{34}$$

Note also, that we have made explicit the isoscalar ($I=0$) and isovector ($I=1$) parts. The wave function implicitly depends on x because $\widetilde{\psi}_v(\boldsymbol{p}_\pm)=\widetilde{\psi}_v(p,\Theta_p^\pm,\Phi)$ where the polar angle $\Theta_p^\pm$ between $\boldsymbol{p}_\pm$ and $\boldsymbol{q}$ is fixed for a given value of the Bjorken scaling variable x.

Turning to the evaluation of the nucleon matrix elements defined above we first note that the Fourier transform of the

wave function is easily obtained because the angular parts are tensor spherical harmonics in both coordinate and momentum spaces. Hence, only the radial part requires numerical treatment. Performing straightforwardly the azimuthal integrations in Eqs. (29) and (30) reveals that the surviving isoscalar part of the longitudinal structure function $g_1^{I=0}$ is linear in the angular velocity $\mathbf{\Omega}$. It is this part which is associated with the proton-spin puzzle. Using the standard quantization condition, $\mathbf{\Omega}=\boldsymbol{J}/\alpha^2$, where α^2 is the moment of inertia of the soliton and further noting that the $\hat{\mathbf{z}}$ direction is distinct, the required nucleon matrix elements are $\langle N,\frac{1}{2}\hat{\mathbf{z}}|J_z|N,\frac{1}{2}\hat{\mathbf{z}}\rangle=\frac{1}{2}$. Thus, $g_1^{I=0}$ is identical for all nucleon states. Choosing a symmetric ordering [54,55] for the noncommuting operators, $D_{ia}J_j\rightarrow\frac{1}{2}\{D_{ia},J_j\}$, we find that the nucleon matrix elements associated with the cranking portion of the isovector piece, $\langle N,\pm\frac{1}{2}\hat{\mathbf{z}}|\{D_{3y},J_x\}|N,\pm\frac{1}{2}\hat{\mathbf{z}}\rangle$, vanish. With this ordering we avoid the occurrence of PCAC (partial conservation of axial-vector current)-violating pieces in the axial-vector current. The surviving terms stem solely from the classical part of the valence quark wave function $\Psi_v(\boldsymbol{x})$ in combination with the collective Wigner-D function D_{3z}. Again, singling out the $\hat{\mathbf{z}}$ direction, the nucleon matrix elements become [19]

$$\langle N,\tfrac{1}{2}\hat{\mathbf{z}}|D_{3z}|N,\tfrac{1}{2}\hat{\mathbf{z}}\rangle=-\tfrac{2}{3}i_3, \tag{35}$$

where $i_3=\pm\frac{1}{2}$ is the nucleon isospin. For the transverse structure function, the surviving piece of the isoscalar contribution is again linear in the angular velocities. The transversally polarized nucleon gives rise to the matrix elements, $\langle N,\frac{1}{2}\hat{\boldsymbol{x}}|J_x|N,\frac{1}{2}\hat{\boldsymbol{x}}\rangle=\frac{1}{2}$. Again, choosing symmetric ordering for terms arising from the cranking contribution, the nucleon matrix elements $\langle N,\frac{1}{2}\hat{\boldsymbol{x}}|\{D_{3y},J_y\}|N,\frac{1}{2}\hat{\boldsymbol{x}}\rangle$ and $\langle N,\frac{1}{2}\hat{\boldsymbol{x}}|\{D_{33},J_y\}|N,\frac{1}{2}\hat{\boldsymbol{x}}\rangle$ vanish. As in the longitudinal case, there is a surviving isovector contribution stemming solely from the classical part of the valence quark wave function $\Psi_v(\boldsymbol{x})$ in combination with the collective Wigner-D function D_{3x}. Now, singling out the $\hat{\boldsymbol{x}}$ direction, the relevant nucleon matrix elements become [19]

$$\langle N,\tfrac{1}{2}\hat{\boldsymbol{x}}|D_{3x}|N,\tfrac{1}{2}\hat{\boldsymbol{x}}\rangle=-\tfrac{2}{3}i_3. \tag{36}$$

Explicit expressions in terms of the valence quark wave functions (33) and (34) for $g_{1,\pm}^{I=0}(x),g_{1,\pm}^{I=1}(x),g_{2,\pm}^{I=0}(x)$, and $g_{,\pm}^{I=1}(x)$ are listed in Appendix A.

Using the expressions given in Appendix A it is straightforward to verify the Bjorken sum rule [47]

$$\Gamma_1^p-\Gamma_1^n=\int_0^1 dx[g_1^p(x)-g_1^n(x)]=g_A/6, \tag{37}$$

the Burkhardt-Cottingham sum rule [48]

$$\Gamma_2^p=\int_0^1 dx g_2^p(x)=0, \tag{38}$$

as well as the axial singlet charge

$$\Gamma_1^p+\Gamma_1^n=\int_0^1 dx[g_1^p(x)+g_1^n(x)]=g_A^0, \tag{39}$$

in this model calculation when the moment of inertia α^2, as well as the axial charges g_A^0 and g_A, are confined to their dominating valence quark pieces. We have used

$$g_A=-\frac{N_C}{3}\int d^3r\,\overline{\psi_v^{\dagger}}(\boldsymbol{r})\gamma_3\gamma_5\tau_3\psi_v(\boldsymbol{r}), \tag{40}$$

$$g_A^0=\frac{N_C}{\alpha_v^2}\int d^3r\,\overline{\psi_v^{\dagger}}(\boldsymbol{r})\gamma_3\gamma_5\psi_v(\boldsymbol{r}), \tag{41}$$

to verify the Bjorken sum rule as well as the axial singlet charge. This serves as an analytic check on our treatment. Here α_v^2 refers to the valence quark contribution to the moment of inertia, i.e., $\alpha_v^2=(1/2)\Sigma_{\mu\neq v}|\langle\mu|\tau_3|v\rangle|^2/(\epsilon_\mu-\epsilon_v)$. The restriction to the valence quark piece is required by consistency with the Adler sum rule in the calculation of the unpolarized structure functions in this approximation [49].

V. NUMERICAL RESULTS

In this section we display the results of the spin–polarized structure functions calculated from Eqs. (A13)–(A16) for constituent quark masses of $m=400$ MeV and 450 MeV. In addition to checking the above mentioned sum rules, see Eqs. (37)–(39), we have numerically calculated the first moment of $g_1^p(x,\mu^2)$,[3]

$$\Gamma_1^p=\int_0^1 dx g_1^p(x), \tag{42}$$

and the Efremov-Teryaev-Leader (ETL) sum rule [52]

$$\Gamma_{\mathrm{ELT}}=\int_0^1 dx x[g_1^p(x)+2g_2^n(x)]. \tag{43}$$

We summarize the results for the sum rules in Table I. When comparing these results with the experimental data one observes two shortcomings, which are already known from studies of the static properties in this model. First, the axial charge $g_A\approx 0.73$ comes out too low as the experimental value is $g_A=1.25$. It has recently been speculated that a different ordering of the collective operators $D_{ai}J_j$ (cf. Sec. IV) may fill the gap [53,45]. However, since such an ordering unfortunately gives rise to PCAC-violating contributions to the axial-vector current [54], and furthermore inconsistencies with G parity may occur in the valence quark approximation [55], we will not pursue this issue any further at this time. Second, the predicted axial singlet charge $g_A^0\approx 0.6$ is approximately twice as large as the number extracted

[3]Which, in this case, amounts to the Ellis-Jaffe sum rule [50] since we have omitted the strange degrees of freedom. A careful treatment of symmetry-breaking effects indicates that the role of the strange quarks is less important than originally assumed [14,51].

TABLE I. Sum rules calculated from Eqs. (38) and (39) as functions of the constituent quark mass m in the NJL-chiral soliton model.

	m (MeV)	400	450
Burkhardt-Cottingham:	Γ_2^p	0	0
Bjorken:	$\Gamma_1^p-\Gamma_1^n=g_A/6$	0.121	0.118
Ellis–Jaffe:	Γ_1^p	0.149	0.139
ETL:	$\Gamma_{\rm ETL}$	1.38×10^{-2}	7.65×10^{-3}
Axial singlet charge:	$\Gamma_1^p+\Gamma_1^n=g_A^0$	0.638	0.579

from experiment[4] 0.27 ± 0.04 [17]. This can be traced back to the valence quark approximation as there are direct and indirect contributions to g_A^0 from both the polarized vacuum and the valence quark level. Before canonical quantization of the collective coordinates one finds a sum of valence and vacuum pieces

$$g_A^0=2(g_v^0+g_{\rm vac}^0)\Omega_3=\frac{g_v^0+g_{\rm vac}^0}{\alpha_v^2+\alpha_{\rm vac}^2}. \tag{44}$$

Numerically, the vacuum piece is negligible, i.e., $g_{\rm vac}^0/g_v^0\approx2\%$. Canonical quantization subsequently involves the moment of inertia $\alpha^2=\alpha_v^2+\alpha_{\rm vac}^2$, which also has valence and vacuum pieces. In this case, however, the vacuum part is not so small: $\alpha_{\rm vac}^2/\alpha^2\approx25\%$. Hence, the full treatment of the polarized vacuum will drastically improve the agreement with the empirical value for g_A^0. On the other hand, our model calculation nicely reproduces the Ellis–Jaffe sum rule since the empirical value is 0.136. Note that this comparison is legitimate since neither the derivation of this sum rule nor our model implies strange quarks. While the vanishing Burkhardt-Cottingham sum rule can be shown analytically in this model, the small value for the Efremov-Teryaev-Leader sum rule is a numerical prediction. Recently, it has been demonstrated [23] that the ETL sum rule (43), which is derived within the parton model, neither vanishes in the center-of-mass bag model nor is supported by the SLAC E143 data [2]. This is also the case for our NJL-model calculation as can be seen from Table I.

In Fig. 1 we display the spin-structure functions $g_1^p(x,\mu^2)$ and $g_2^p(x,\mu^2)$ along with the twist-two piece $g_2^{\rm WW(p)}(x,\mu^2)$ and twist-three piece $\overline{g_2^p}(x,\mu^2)$. The actual value for μ^2 and the precise definition of the twist-two and twist-three pieces [see Eqs. (48) and (49)] will be given in the following section in the context of the evolution procedure. We observe that the structure functions $g_2^p(x,\mu^2)$ and $g_2^{\rm WW(p)}(x,\mu^2)$ are well localized in the interval $0\leqslant x\leqslant1$, while for g_1^p about 0.3% of the first moment, $\Gamma_1^p=\int_0^1dx\,g_1^p(x,\mu^2)$ comes from the region $x>1$. The polarized structure function $g_1^p(x,\mu^2)$ exhibits a pronounced maximum at $x\approx0.3$ which is smeared out when the constituent quark mass increases. This can be understood as follows: In our chiral soliton model the constituent mass serves as a coupling constant of the quarks to the chiral field [see Eqs. (7) and (10)]. The valence quark becomes more strongly bound as the constituent quark mass increases. In this case the lower components of the valence quark wave function increase and relativistic effects become more important resulting in a broadening of the maximum. With regard to the Burkhardt-Cottingham sum rule the polarized structure function $g_2^p(x,\mu^2)$ possesses a node. Apparently, this node appears at approximately the same value of the Bjorken variable x as the maximum of $g_1^p(x,\mu^2)$. Note also that the distinct twist contributions to $g_2^p(x,\mu^2)$ by construction diverge as $\ln(x)$ as $x\to0$ while their sum stays finite (see Sec. VI for details).

As the results displayed in Fig. 1 are the central issue of our calculation it is of great interest to compare them with the available data. As for all effective low-energy models of the nucleon, the predicted results are at a lower scale Q^2 than the experimental data. In order to carry out a sensible comparison either the model results have to be evolved upward or the QCD renormalization group equations have to be used to extract structure functions at a low-renormalization point. For the combination $xg_1(x)$ a parametrization of the empirical structure function is available at a low scale [31].[5] In that study the experimental high Q^2 data are evolved to the low-renormalization point μ^2, which is defined as the lowest Q^2 satisfying the positivity constraint between the polarized and unpolarized structure functions. In a next-to-leading order calculation those authors found $\mu^2=0.34$ GeV^2 [31]. In Fig. 2 we compare our results for two different constituent quark masses with that parametrization. We observe that our predictions reproduce gross features such as the position of the maximum. This agreement is more pronounced the lower the constituent quark is, i.e., the agreement improves as the applicability of the valence quark approximation becomes more justified. Unfortunately, such a parametrization is currently not available for the transverse structure function $g_T(x)$ [or $g_2(x)$]. In order to, nevertheless, be able to compare our corresponding results with the (few) available data we will apply leading-order evolution techniques to the structure functions calculated in the valence quark approximation to the NJL-soliton model. This will be subject of the following section.

[4]Note that this analysis assumes SU(3) flavor symmetry, which, of course, is not manifest in our two-flavor model.

[5]These authors also provide a low-scale parametrization of quark distribution functions. However, these refer to the distributions of perturbatively interacting partons. Distributions for the NJL-model constituent quarks could in principle be extracted from Eqs. (28)–(31). It is important to stress that these distributions may not be compared to those of Ref. [31] because the associated quarks fields are different in nature.

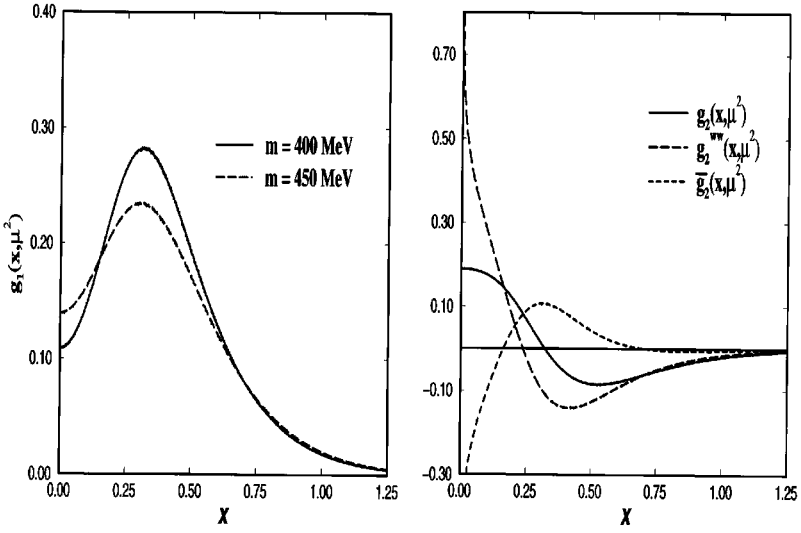

FIG. 1. The valence quark approximation of the polarized proton structure functions as a function of Bjorken x. Left panel: $g_1^p(x,\mu^2)$ for two constituent quark masses m. Right panel: $g_2^p(x,\mu^2)$ (solid line), $g_2^{\mathrm{WW}(p)}(x,\mu^2)$ (long-dashed line) and twist-three portion $\overline{g_2^p}(x,\mu^2)$ (dashed line). In this case we have used $m=400$ MeV.

VI. PROJECTION AND EVOLUTION

One notices that our baryon states are not momentum eigenstates causing the structure functions (see Figs. 1 and 2) not to vanish exactly for $x>1$ although the contributions for $x>1$ are very small. This shortcoming is due to the localized field configuration and thus the nucleon not being a representation of the Poincaré group which is common to the low-energy effective models. The most feasible procedure to cure this problem is to apply Jaffe's prescription [32],

$$f(x)\to\tilde{f}(x)=\frac{1}{1-x}f(-\ln(1-x)), \tag{45}$$

to project any structure function $f(x)$ onto the interval $[0,1]$. In view of the kinematic regime of DIS this prescription, which was derived in a Lorentz-invariant fashion within the $(1+1)$-dimensional bag model, is a reasonable approximation. It is important to note in the NJL model the unprojected nucleon wave function [including the cranking piece,[6] see Eq. (14)] is anything but a product of Dirac spinors. In this context, techniques such as Peierls-Yoccoz [56] (which do not completely enforce proper support [57] $0\leqslant x\leqslant 1$ nor restore Lorentz invariance, see [58]) appear to be infeasible. Thus, given the manner in which the nucleon arises in chiral soliton models, Jaffe's projection technique is quite well suited. It is also important to note that, by construction, sum rules are not effected by this projection, i.e., $\int_0^\infty dx f(x)=\int_0^1 dx\,\tilde{f}(x)$. Accordingly, the sum rules of the previous section remain intact.

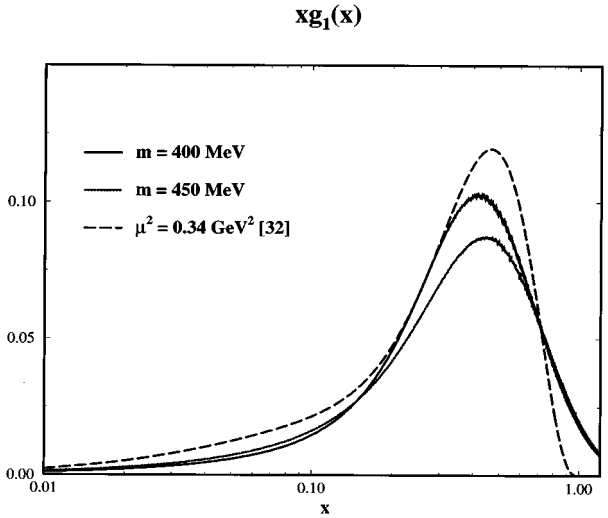

FIG. 2. The valence quark approximation to the nucleon structure function $xg_1(x)$ in the NJL-soliton model compared to the low-renormalization point result of Ref. [31].

With regard to evolution of the spin-polarized structure functions applying the OPE analysis of Sec. II, Jaffe and Ji brought to light that, to leading order in $1/Q^2$, $g_1(x,Q^2)$ receives only a leading order twist-two contribution, while $g_2(x,Q^2)$ possesses contributions from both twist-two and twist-three operators; the twist-three portion coming from spin-dependent gluonic quark correlations [36,40] (see also [59,60]). In the *impulse approximation* [36,40,41] these leading contributions are given by

$$\lim_{Q^2\to\infty}\int_0^1 dx x^n g_1(x,Q^2)=\frac{1}{2}\sum_i O_{2,i}^n,\quad n=0,2,4,\ldots, \tag{46}$$

$$\lim_{Q^2\to\infty}\int_0^1 dx x^n g_2(x,Q^2)=-\frac{n}{2(n+1)}\sum_i\{O_{2,i}^n-O_{3,i}^n\},\quad n=2,4,\ldots. \tag{47}$$

Note that there is no sum rule for the first moment, $\Gamma_2(Q^2)=\int_0^1 dx g_2(x,Q^2)$ [36]. Some time ago, Wandzura and Wilczek (WW) [61] proposed that $g_2(x,Q^2)$ was given in terms of $g_1(x,Q^2)$,

$$g_2^{\mathrm{WW}}(x,Q^2)=-g_1(x,Q^2)+\int_x^1\frac{dy}{y}g_1(y,Q^2), \tag{48}$$

[6]Which, in fact, yields the leading order to the Adler sum rule $F_1^{\nu p}-F_1^{\bar{\nu}p}$ [49], rather than being a correction.

which follows immediately from Eqs. (46) and (47) by neglecting the twist-three portion in the sum in Eq. (47). One may reformulate this argument to extract the twist-three piece

$$\overline{g_2}(x,Q^2)=g_2(x,Q^2)-g_2^{\rm WW}(x,Q^2), \tag{49}$$

since,

$$\int_0^1 dx x^n \overline{g_2}(x,Q^2)=\frac{n}{2(n+1)}\sum_i O_{3,i}^n, \quad n=2,4,\ldots. \tag{50}$$

In the NJL model as in the bag model there are no explicit gluon degrees of freedom, however, in both models twist-three contributions to $g_2(x,\mu^2)$ exist. In contrast with the bag model where the bag boundary simulates the quark-gluon and gluon-gluon correlations [23] in the NJL model, the gluon degrees of freedom, having been ''integrated'' out, leave correlations characterized by the four-point quark coupling $G_{\rm NJL}$. This is the source of the twist-three contribution to $g_2(x,\mu^2)$, which is shown in Fig. 1.

For $g_1(x,Q^2)$ and the twist-two piece $g_2^{\rm WW}(x,Q^2)$ we apply the leading order [in $\alpha_{\rm QCD}(Q^2)$] Altarelli-Parisi equations [33] to evolve the structure functions from the model scale μ^2 to that of the experiment Q^2, by iterating

$$g(x,t+\delta t)=g(x,t)+\delta t\frac{dg(x,t)}{dt}, \tag{51}$$

where $t=\ln(Q^2/\Lambda^2_{\rm QCD})$. The explicit expression for the evolution differential equation is given by the convolution integral,

$$\begin{aligned}\frac{dg(x,t)}{dt}&=\frac{\alpha(t)}{2\pi}g(x,t)\otimes P_{qq}(x)\\&=\frac{\alpha(t)}{2\pi}C_R(F)\int_x^1\frac{dy}{y}P_{qq}(y)g\left(\frac{x}{y},t\right),\end{aligned} \tag{52}$$

where the quantity $P_{qq}(z)=[(1+z^2)/(1-z^2)]_+$ represents the quark probability to emit a gluon such that the momentum of the quark is reduced by the fraction z. $C_R(f)=(n_f^2-1)/2n_f$ for n_f flavors, $\alpha_{\rm QCD}=4\pi/[\beta\ln(Q^2/\Lambda^2)]$ and $\beta=(11-\frac{2}{3}n_f)$. Employing the ''+'' prescription [34] yields

$$\begin{aligned}\frac{dg(x,t)}{dt}=\frac{2C_R(f)}{9t}\Bigg\{&\left(x+\frac{x^2}{2}+2\ln(1-x)\right)g(x,t)\\&+\int_x^1 dy\left(\frac{1+y^2}{1-y}\right)\left[\frac{1}{y}g\left(\frac{x}{y},t\right)-g(x,t)\right]\Bigg\}.\end{aligned} \tag{53}$$

As discussed in Sec. II the initial value for integrating the differential equation is given by the scale μ^2 at which the model is defined. It should be emphasized that this scale essentially is a new parameter of the model. For a given constituent quark mass we fit μ^2 to maximize the agreement of the predictions with the experimental data on previously [49] calculated unpolarized structure functions for (anti)neutrino-proton scattering: $F_2^{\nu p}-F_2^{\overline{\nu p}}$. For the constituent quark mass $m=400$ MeV we have obtained $\mu^2\approx 0.4$ GeV^2. One certainly wonders whether for such a low scale the restriction to first order in $\alpha_{\rm QCD}$ is reliable. There are two answers. First, the studies in this section aim at showing that the required evolution indeed improves the agreement with the experimental data and, second, in the bag model it has recently been shown [62] that a second-order evolution just increases μ^2 without significantly changing the evolved data. In Fig. 3 we compare the unevolved, projected, structure function $g_1^p(x,\mu^2)$ with the one evolved from $\mu^2=0.4$ GeV^2 to $Q^2=3.0$ GeV^2. Also, the data from the E143 Collaboration from SLAC [7] are given. Furthermore, in Fig. 3 we compare the projected, unevolved, structure function $g_2^{{\rm WW}(p)}(x,\mu^2)$ as well as the one evolved to $Q^2=5.0$ GeV^2 with the data from the recent E143 Collaboration at SLAC [2]. As expected, we observe that the evolution pronounces the structure function at low x; thereby improving the agreement with the experimental data. This change towards small x is a general feature of the projection and evolution process and presumably not very sensitive to the prescription applied here. In particular, choosing an alternative projection technique may easily be compensated by an appropriate variation of the scale μ^2.

While the evolution of the structure function $g_1(x,Q^2)$ and the twist-two piece $g_2^{\rm WW}(x,Q^2)$ from μ^2 to Q^2 can be performed straightforwardly using the ordinary Altarelli-Parisi equations, this is not the case for the twist-three piece $\overline{g_2}(x,Q^2)$. As the twist-three quark and quark-gluon operators mix, the number of independent operators contributing to the twist-three piece increases with n, where n refers to the nth moment [60]. We apply an approximation (see Appendix B) suggested in [35] where it is demonstrated that in $N_c\to\infty$ limit the quark operators of twist three decouple from the evolution equation for the quark-gluon operators of the same twist resulting in a unique evolution scheme. This scheme is particularly suited for the NJL-chiral soliton model, as the soliton picture for baryons is based on $N_c\to\infty$ arguments.[7]

In Fig. 4 we compare the projected, unevolved, structure function $\overline{g_2^p}(x,\mu^2)$ evolved to $Q^2=5.0$ GeV^2 using the scheme suggested in [35]. In addition, we reconstruct $g_2^p(x,Q^2)$ at $Q^2=3.0$ GeV^2 from $g_2^{{\rm WW}(p)}(x,Q^2)$ and $\overline{g_2}(x,Q^2)$ and compare it with the recent SLAC data [2] for $g_2^p(x,Q^2)$. As is evident, our model calculation of $g_2^p(x,Q^2)$, built up from its twist-two and twist-three pieces, agrees reasonably well with the data although the experimental errors are quite large.

VII. SUMMARY AND OUTLOOK

In this paper we have presented the calculation of the polarized nucleon structure functions $g_1(x,Q^2)$ and $g_2(x,Q^2)$ within a model which is based on chiral symmetry and its spontaneous breaking. Specifically, we have em-

[7]This scheme has also been employed by Song [23] in the center-of-mass bag model.

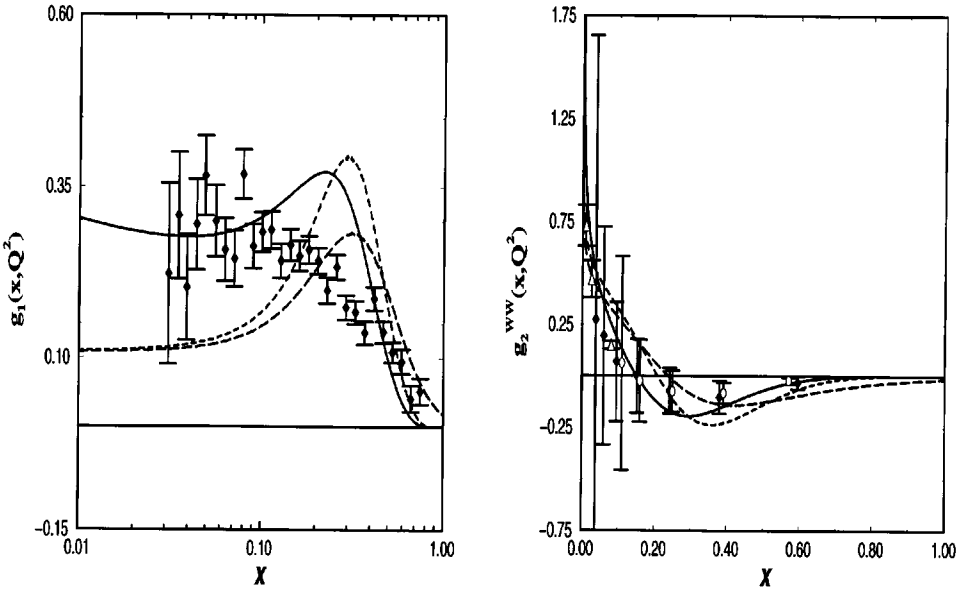

FIG. 3. The projection and evolution of the spin-polarized structure functions as a function of Bjorken x. For the constituent quark mass we choose $m=400$ MeV. Left panel: $g_1^p(x,Q^2)$, unprojected (long-dashed line), projected (dashed line), and evolved from $\mu=0.4$ GeV^2 to $Q^2=3.0$ GeV^2 (solid line). Data are from [7]. Right panel: $g_2^{WW(p)}(x,Q^2)$, unprojected (long-dashed line), projected (dashed line), and evolved from $\mu=0.4$ GeV^2 to $Q^2=5.0$ GeV^2 (solid line). Data are from [2,5], where the diamonds, circles, and triangles correspond to the 4.5° E143, 7.0° E143, and SMC kinematics, respectively. Overlapping data have been shifted slightly in x. The statistical errors are displayed.

ployed the NJL-chiral soliton model which reasonably describes the static properties of the nucleon [26,45]. In this model the current operator is formally identical to the one in a noninteracting relativistic quark model. While the quark fields become functionals of the chiral soliton upon bosonization, this feature enables one to calculate the hadronic tensor. From this hadronic tensor we have then extracted the polarized structure functions within the valence quark approximation. As the explicit occupation of the valence quark level yields the major contribution (about 90%) to the associated static quantities such as the axial charge, this presumably is a justified approximation. When cranking corrections are included this share may be reduced, depending on whether or not the full moment of inertia is substituted.

It needs to be stressed that in contrast with, e.g., bag models, the nucleon wave function arises as a collective excitation of a nonperturbative meson field configuration. In particular, the incorporation of chiral symmetry leads to the distinct feature that the pion field cannot be treated perturbatively. Because of the hedgehog structure of this field one starts with grand spin symmetric quark wave functions rather than direct products of spatial spinors and isospinors as in the bag model. On top of these grand spin wave functions one has to include cranking corrections to generate states with the correct nucleon quantum numbers. Not only are these corrections sizable but even more importantly one would not be able to make any prediction on the flavor singlet combination of the polarized structure functions without them. The structure functions obtained in this manner are, of course, characterized by the scale of the low-energy effective model. We have confirmed this issue by obtaining a reason-

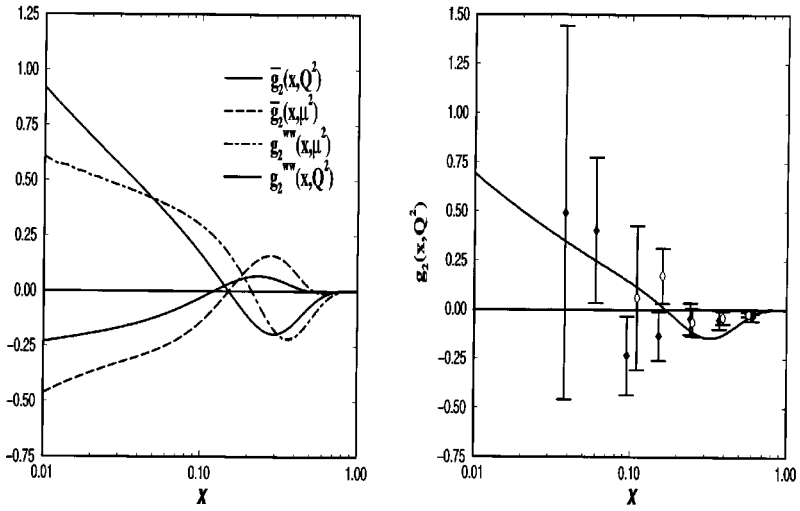

FIG. 4. The evolution of $\overline{g_2^p}(x,Q^2)$ (projected) from $\mu=0.4$ GeV^2 (long-dashed line) to $Q^2=5.0$ GeV^2 (solid line). In addition, we display the corresponding evolution for $g_2^{WW(p)}(x,Q^2)$ (projected). Right panel, $g_2^p(x,Q^2)=g_2^{WW(p)}(x,Q^2)+\overline{g_2^p}(x,Q^2)$ evolved from $\mu^2=0.4\text{GeV}^2$ to $Q^2=5.0$ GeV^2. Data and statistical errors for $g_2^p(x,Q^2)$ are displayed from [2], where the diamonds and circles correspond to the 4.5° E143 and 7.0° E143 kinematics, respectively. Overlapping data have been slightly shifted in x.

able agreement of the model predictions for the structure function g_1 of the proton with the low-renormalization point parametrization of Ref. [31]. In general, this scale of the effective model essentially represents an intrinsic parameter of a model. For the NJL-soliton model we have previously determined this parameter from the behavior of the unpolarized structure functions under the Altarelli-Parisi evolution [49]. Applying the same procedure to the polarized structure functions calculated in the NJL model yields good agreement with the data extracted from experiment, although the error bars on $g_1(x,Q^2)$ are still sizable. In particular, the good agreement at low x indicates that to some extend gluonic effects are already incorporated in the model. This can be understood by noting that the quark fields, which enter our calculation, are constituent quarks. They differ from the current quarks by a mesonic cloud which contains gluonic components. Furthermore, the existence of gluonic effects in the model would not be astonishing because we had already observed from the nonvanishing twist-three part of $g_2(x,Q^2)$, which in the OPE is associated with the quark-gluon interaction, that the model contains the main features allocated to the gluons.

There is a wide avenue for further studies in this model. Of course, one would like to incorporate the effects of the polarized vacuum, although one expects from the results on the static axial properties that their direct contributions are negligible. It may be more illuminating to include the strange quarks within the valence quark approximation. This extension of the model seems to be demanded by the analysis of the proton-spin puzzle. Technically, two changes will occur. First, the collective matrix elements will be more complicated than those in Eqs. (35) and (36) because the nucleon wave functions will be distorted SU(3)-D functions in the presence of flavor symmetry breaking [63,16]. Furthermore, the valence quark wave function (14) will contain an additional correction due to different nonstrange and strange constituent quark masses [64]. When these corrections are included, direct information will be obtained on the contributions of the strange quarks to polarized nucleon structure functions. In particular, the previously developed generalization to three flavors [64] allows one to consistently include the effects of flavor symmetry breaking.

ACKNOWLEDGMENTS

This work was supported in part by the Deutsche Forschungsgemeinschaft (DFG) under Contract No. Re 856/2-2. L.G. is grateful for helpful comments by G. R. Goldstein.

APPENDIX A: SPIN-POLARIZED STRUCTURE FUNCTIONS

In this appendix we summarize the explicit expressions for the structure functions, Eqs. (29)–(32). The first step is to construct the eigenfunctions of the single-particle Dirac Hamiltonian (10) in coordinate space. As the hedgehog ansatz (9) connects coordinate space with isospace, these eigenfunctions are also eigenstates of the grand spin operator

$$\boldsymbol{G}=\boldsymbol{J}+\frac{\boldsymbol{\tau}}{2}=\boldsymbol{l}+\frac{\boldsymbol{\sigma}}{2}+\frac{\boldsymbol{\tau}}{2}, \tag{A1}$$

which is the sum of the total spin $\boldsymbol{J}$ and the isospin $\boldsymbol{\tau}/2$. The spin itself is decomposed into orbital angular momentum $\boldsymbol{l}$ and intrinsic spin $\boldsymbol{\sigma}/2$. Denoting by M the grand spin projection quantum number, the tensor spherical harmonics which are associated with the grand spin may be written as $\mathcal{Y}^{G,M}_{l,j}(\hat{\boldsymbol{r}})$. Note that these tensor spherical harmonics are two-component spinors in both spin and isospin spaces. Given a fixed profile function $\Theta(r)$ the numerical diagonalization of the Dirac Hamiltonian (10) yields the radial functions $g^{(G,+,1)}_{\mu}(r), f^{(G,+,1)}_{\mu}(r)$, etc., in (cf. Ref. [65])

$$\Psi^{(G,+)}_{\mu}(\boldsymbol{r})=\begin{pmatrix} ig^{(G,+;1)}_{\mu}(r)\mathcal{Y}^{G,M}_{G,G+1/2}(\hat{\boldsymbol{r}}) \\ f^{(G,+;1)}_{\mu}(r)\mathcal{Y}^{G,M}_{G+1,G+1/2}(\hat{\boldsymbol{r}}) \end{pmatrix} + \begin{pmatrix} ig^{(G,+;2)}_{\mu}(r)\mathcal{Y}^{G,M}_{G,G-1/2}(\hat{\boldsymbol{r}}) \\ -f^{(G,+;2)}_{\mu}(r)\mathcal{Y}^{G,M}_{G-1,G-1/2}(\hat{\boldsymbol{r}}) \end{pmatrix}, \tag{A2}$$

$$\Psi^{(G,-)}_{\mu}(\boldsymbol{r})=\begin{pmatrix} ig^{(G,-;1)}_{\mu}(r)\mathcal{Y}^{G,M}_{G+1,G+1/2}(\hat{\boldsymbol{r}}) \\ -f^{(G,-;1)}_{\mu}(r)\mathcal{Y}^{G,M}_{G,G+1/2}(\hat{\boldsymbol{r}}) \end{pmatrix} + \begin{pmatrix} ig^{(G,-;2)}_{\mu}(r)\mathcal{Y}^{G,M}_{G-1,G-1/2}(\hat{\boldsymbol{r}}) \\ f^{(G,-;2)}_{\mu}(r)\mathcal{Y}^{G,M}_{G,G-1/2}(\hat{\boldsymbol{r}}) \end{pmatrix}. \tag{A3}$$

The second superscript $(\pm)$ denotes the intrinsic parity, which also is a conserved quantum number.[8] Note that for the $G=0$ channel, which contains the classical contribution to the valence quark wave function in Eq. (14),

$$\Psi_{v}(\boldsymbol{r})=\begin{pmatrix} ig_{v}(r)\mathcal{Y}^{0,0}_{0,1/2}(\hat{\boldsymbol{r}}) \\ f_{v}(r)\mathcal{Y}^{0,0}_{1,1/2}(\hat{\boldsymbol{r}}) \end{pmatrix}, \tag{A4}$$

only the components with $j=+1/2$ are allowed. In addition to the classical piece (A4), the complete valence quark wave function (14) also contains the cranking correction, which dwells in the channel with $G=1$ and negative intrinsic parity.

The discretization (μ) is accomplished by choosing suitable boundary conditions at a radial distance which is large compared to the soliton extension [65,64]. This calculation yields the energy eigenvalues ϵ_{μ}, which enter the energy functional (11). The soliton configuration is finally determined by self-consistently minimizing this energy functional. In Ref. [66] the numerical procedure is described in detail.

We continue by making explicit the Fourier transform (27) of Eq. (14):

$$\widetilde{\psi}_{v}(\boldsymbol{p})=\widetilde{\Psi}_{v}(\boldsymbol{p})+Q_{\mu}\widetilde{\Psi}_{\mu}(\boldsymbol{p}). \tag{A5}$$

The leading order in N_c valence quark contribution is just the Fourier transform of Eq. (A5),

[8]The total parity is given by the product of the intrinsic parity and $(-)^G$.

$$\widetilde{\Psi}_v(\boldsymbol{p}) = i\begin{pmatrix} \widetilde{g}_v(p)\mathcal{Y}^{0,0}_{0,1/2}(\hat{\boldsymbol{p}}) \\ \widetilde{f}_v(p)\mathcal{Y}^{0,0}_{1,1/2}(\hat{\boldsymbol{p}}) \end{pmatrix}, \tag{A6}$$

and the cranking correction involves the Fourier transform of spinor with $G=1$ and negative intrinsic parity:

$$\widetilde{\Psi}_\mu(\boldsymbol{p}) = -i\begin{pmatrix} \widetilde{g}^{(1)}_\mu(p)\mathcal{Y}^{1,M}_{2,3/2}(\hat{\boldsymbol{p}}) - \widetilde{g}^{(2)}_\mu(p)\mathcal{Y}^{1,M}_{0,1/2}(\hat{\boldsymbol{p}}) \\ \widetilde{f}^{(1)}_\mu(p)\mathcal{Y}^{1,M}_{1,3/2}(\hat{\boldsymbol{p}}) - \widetilde{f}^{(2)}_\mu(p)\mathcal{Y}^{1,M}_{1,1/2}(\hat{\boldsymbol{p}}) \end{pmatrix}. \tag{A7}$$

Here $\mathcal{Y}^{G,M}_{l,j}(\hat{\boldsymbol{p}})$ are the Fourier transforms of the tensor spherical harmonics associated with the grand spin operator (A1). The Fourier transform for the radial functions is defined by

$$\widetilde{\phi}_\mu(p) = \int_0^R dr r^2 j_l(pr)\phi_\mu(r). \tag{A8}$$

Here the index l of the Bessel function denotes the orbital angular momentum of the associated tensor spherical harmonic in Eqs. (A6) and (A7). We have suppressed the grand spin index on the transforms of the radial wave functions for convenience. For purposes of notation we have introduced the quantity Q_μ which arises in analyzing the matrix elements [see Eq. (14)]:

$$\frac{\langle\mu|\boldsymbol{\tau}\cdot\boldsymbol{\Omega}|v\rangle}{\epsilon_v-\epsilon_\mu} = Q_\mu\left\{\frac{\delta_{M,1}}{\sqrt{2}}(\Omega_1+\Omega_2) - \frac{\delta_{M,-1}}{\sqrt{2}}(\Omega_1-\Omega_2) - \delta_{M,0}\Omega_0\right\}\delta_{G_\mu,1}, \tag{A9}$$

where

$$Q_\mu \equiv \frac{1}{\epsilon_v-\epsilon_\mu}\int dr r^2\{g_v(r)g^{(2)}_\mu(r) + f_v(r)f^{(2)}_\mu(r)\}. \tag{A10}$$

Defining the combinations

$$\widetilde{f}^{(i)}(p) = Q_\mu\widetilde{f}^{(i)}_\mu(p), \tag{A11}$$

$$\widetilde{g}^{(i)}(p) = Q_\mu\widetilde{g}^{(i)}_\mu(p), \quad i=1,2, \tag{A12}$$

the isoscalar (vector) contributions to the spin-polarized structure functions, Eqs. (29)–(32), read

$$g^{I=0}_{1,\pm}(x,\mu^2) = -N_C\frac{5M_N}{36\pi}\int_{M_N|x_\mp|}^\infty pdp\left\{\widetilde{g}_v(p)\widetilde{g}^{(1)}(p)\frac{1-3\cos^2(\Theta^\pm_p)}{\sqrt{8}} - \frac{1}{2}\widetilde{g}_v(p)\widetilde{g}^{(2)}(p) \mp \widetilde{g}_v(p)\widetilde{f}^{(1)}(p)\frac{\cos(\Theta^\pm_p)}{\sqrt{2}}\right.$$
$$\mp\widetilde{g}_v(p)\widetilde{f}^{(2)}(p)\frac{\cos(\Theta^\pm_p)}{2} \mp \widetilde{f}_v(p)\widetilde{g}^{(1)}(p)\frac{\cos(\Theta^\pm_p)}{\sqrt{2}} \mp \widetilde{f}_v(p)\widetilde{g}^{(2)}(p)\frac{\cos(\Theta^\pm_p)}{2} - \widetilde{f}_v(p)\widetilde{f}^{(1)}(p)\frac{1+\cos^2(\Theta^\pm_p)}{\sqrt{8}}$$
$$\left.+\widetilde{f}_v(p)\widetilde{f}^{(2)}(p)\frac{1-2\cos^2(\Theta^\pm_p)}{2}\right\}, \tag{A13}$$

$$g^{I=1}_{1,\pm}(x,\mu^2) = -N_C\frac{M_N}{36\pi}\int_{M_N|x_\mp|}^\infty pdp\{\widetilde{g}_v(p)^2 \pm 2\widetilde{g}_v(p)\widetilde{f}_v(p)\cos(\Theta^\pm_p) - \widetilde{f}_v(p)^2[1-2\cos^2(\Theta^\pm_p)]\}, \tag{A14}$$

$$g^{I=0}_{T,\pm}(x,\mu^2) = -N_C\frac{5M_N}{36\pi}\int_{M_N|x_\mp|}^\infty pdp\left\{\widetilde{g}_v(p)\widetilde{g}^{(1)}(p)\frac{3\cos^2(\Theta^\pm_p)-1}{4\sqrt{2}} - \frac{1}{2}\widetilde{g}_v(p)\widetilde{g}^{(2)}(p) \mp \widetilde{g}_v(p)\widetilde{f}^{(1)}(p)\frac{\cos^2(\Theta^\pm_p)-3}{4\sqrt{2}}\right.$$
$$\left.+\widetilde{f}_v(p)\widetilde{f}^{(2)}(p)\frac{\cos^2(\Theta^\pm_p)}{2}\right\}, \tag{A15}$$

$$g^{I=1}_{T,\pm}(x,\mu^2) = -N_C\frac{M_N}{36\pi}\int_{M_N|x_\mp|}^\infty pdp\{\widetilde{g}_v(p)^2 - \widetilde{f}_v(p)^2\cos^2(\Theta^\pm_p)\}, \tag{A16}$$

which we evaluate numerically. Note that in case of the neutron the signs of the isovector pieces have to be reversed. Note that the angle $\Theta^\pm_p$ is related to the integration variable p via

$$\cos\Theta^\pm_p = \frac{1}{p}|M_N x \mp \epsilon_v|. \tag{A17}$$

In Ref. [67] the structure function g_1 was calculated omitting the cranking corrections. In the special case of the isovector component these corrections drop out and we formally confirm the result displayed in Eq. (B.6) of Ref. [67].

APPENDIX B: EVOLUTION OF $\overline{g_2}(x,\mu^2)$

In the $N_c\to\infty$ limit it has been shown [36] that one can evolve the moments of $\overline{g_2}(x,\mu^2)$,

$$M_j(Q^2)=\left(\frac{\alpha_s(Q^2)}{\alpha_s(\mu^2)}\right)^{(\gamma_{j-1})/b} M_j(\mu^2) \tag{B1}$$

from the scale μ^2 to Q^2, where the anomalous dimensions are

$$\gamma_{j-1}=2N_c\left(\psi(j)+\frac{1}{2j}+\gamma_{\rm E}-\frac{1}{4}\right), \tag{B2}$$

with $\psi(x)=(d/dx)\ln\Gamma(x)$ and $b=(11N_c-2n_f)/3$. N_c and n_f are the number of colors and flavors, respectively. Given the moments of $\overline{g_2}(x,\mu^2)$,

$$M_j(\mu^2)=\int_0^1 dx x^{j-1}\overline{g_2}(x,\mu^2), \tag{B3}$$

and expressing $\overline{g_2}(x,\mu^2)$ in terms of the $\ln(x)$ and a power series in x,

$$\overline{g_2}(x,\mu^2)=a_1(\mu^2)\ln(x)+\sum_{n=0}^{\infty} a_n(\mu^2)x^n, \tag{B4}$$

one can alternatively express the moments M_j in terms of the coefficients a_n

$$M_j(\mu^2)=A_{jn}a_n(\mu^2). \tag{B5}$$

We calculate the moments $M_j(\mu^2)$ from Eq. (B3) and evolve them according to Eq. (B1). Finally, inverting the matrix A_{jn}, we obtain the evolved coefficients $a_n(Q^2)$ which in turn yield $\overline{g_2}(x,Q^2)$ (see Fig. 4).

[1] J. Ashman*et al.*, Phys. Lett. B **206**, 364 (1988); Nucl. Phys. **B328**, 1 (1989).
[2] K. Abe *et al.*, Phys. Rev. Lett. **76**, 587 (1996).
[3] B. Adeva *et al.*, Phys. Lett. B **302**, 533 (1993).
[4] D. Adams *et al.*, Phys. Lett. B **329**, 399 (1994).
[5] J. Adams *et al.*, Phys. Lett. B **336**, 125 (1994).
[6] P. L. Anthony *et al.*, Phys. Rev. Lett. **71**, 959 (1993).
[7] K. Abe *et al.*, Phys. Rev. Lett. **74**, 346 (1995).
[8] K. Abe *et al.*, Phys. Rev. Lett. **75**, 25 (1995).
[9] J. J. Kokkedee, *The Quark Model* (Benjamin Press, New York, 1979).
[10] Y. Nambu and G. Jona-Lasinio, Phys. Rev. **122**, 345 (1961); **124**, 246 (1961).
[11] H. Reinhardt and R. Wünsch, Phys. Lett. B **215**, 577 (1988); **230**, 93 (1989); T. Meissner, F. Grümmer, and K. Goeke, *ibid.* **227**, 296 (1989); R. Alkofer, *ibid.* **236**, 310 (1990).
[12] S. Brodsky, J. Ellis, and M. Karliner, Phys. Lett. B **206**, 309 (1988); J. Ellis and M. Karliner, *ibid.* **213**, 73 (1988).
[13] N. W. Park, J. Schechter, and H. Weigel, Phys. Lett. B **224**, 171 (1989).
[14] R. Johnson, N. W. Park, J. Schechter, V. Soni, and H. Weigel, Phys. Rev. D **42**, 2998 (1990).
[15] A. Blotz, M. V. Ployakov, and K. Goeke, Phys. Lett. B **302**, 151 (1993).
[16] H. Weigel, Int. J. Mod. Phys. A **11**, 2419 (1996).
[17] J. Ellis and M. Karliner, ''The Strange Spin of the Nucleon,'' Report No. hep-ph/9601280 (unpublished).
[18] T. H. R. Skyrme, Proc. R. Soc. London **A260**, 127 (1961); for reviews see G. Holzwarth and B. Schwesinger, Rep. Prog. Phys. **49**, 825 (1986); I. Zahed and G. E. Brown, Phys. Rep. **142**, 481 (1986).
[19] G. S. Adkins, C. R. Nappi, and E. Witten, Nucl. Phys. **B228**, 552 (1983).
[20] R. Friedberg and T. D. Lee, Phys. Rev. D **15**, 1694 (1977).
[21] H. B. Nielsen and A. Patkos, Nucl. Phys. **B195**, 137 (1982).
[22] A. Chodos, R. L. Jaffe, K. Johnson, C. B. Thorn, and V. F. Weisskopf, Phys. Rev. D **9**, 3471 (1974); **10**, 2599 (1974); for a review see A. W. Thomas, Adv. Nucl. Phys. **13**, 1 (1982).
[23] X. I. Song and J. S. McCarthy, Phys. Rev. D **49**, 3169 (1994); X. I. Song, *ibid.* **54**, 1955 (1996).
[24] V. Sanjose and V. Vento, Phys. Lett. B **225**, 15 (1988); Nucl. Phys. **A501**, 672 (1989).
[25] A. W. Schreiber, P. J. Mulders, A. I. Signal, and A. W. Thomas, Phys. Rev. D **45**, 3069 (1992).
[26] R. Alkofer, H. Reinhardt, and H. Weigel, Phys. Rep. **265**, 139 (1996).
[27] H. Reinhardt, Nucl. Phys. **A503**, 825 (1989).
[28] R. L. Jaffe, Phys. Rev. D **11**, 1953 (1975); R. L. Jaffe and A. Patrascioiu, *ibid.* **12**, 1314 (1975).
[29] M. Birse and M. K. Banerjee, Phys. Rev. D **31**, 118 (1985); S. Kahana, G. Ripka, and V. Soni, Nucl. Phys. **A415**, 351 (1984); P. Jain, R. Johnson, and J. Schechter, Phys. Rev. D **38**, 1571 (1988); for a review see M. K. Banerjee, W. Broniwoski, and T. D. Cohen, *A Chiral Quark Soliton Model in Chiral Solitons*, edited by K. F. Lui (1986), p. 255.
[30] G. E. Brown and M. Rho, Phys. Lett. **82B**, 177 (1979); V. Vento, M. Rho, E. M. Nyman, J. H. Jun, and G. E. Brown, Nucl. Phys. **A345**, 413 (1980); for a review see A. Hosaka and H. Toki, Phys. Rep. **277**, 65 (1996).
[31] M. Glück, E. Reya, and A. Vogt, Z. Phys. C **67**, 433 (1995); M. Glück, E. Reya, M. Stratmann, and W. Vogelsang, Phys. Rev. D **53**, 4775 (1996); W. Vogelsang, *ibid.* **54**, 2023 (1996).
[32] R. L. Jaffe and G. G. Ross, Phys. Lett. **93B**, 313 (1980); R. L. Jaffe, Ann. Phys. (N.Y.) **132**, 32 (1981).
[33] G. Altarelli and G. Parisi, Nucl. Phys. **B126**, 298 (1977).
[34] G. Altarelli, P. Nason, and G. Ridolfi, Phys. Lett. B **320**, 152 (1994); **320**, 538(E) (1994).
[35] A. Ali, V. M. Braun, and G. Hiller, Phys. Lett. B **266**, 117 (1991).
[36] R. L. Jaffe, Comments Nucl. Part. Phys. **19**, 239 (1990).
[37] T. Muta, *Foundations of Quantum Chromodynamics* (World Scientific, Singapore, 1987).
[38] R. G. Roberts, *The Structure of the Proton* (Cambridge University Press, Cambridge, England, 1990).
[39] M. Anselmino *et al.*, Phys. Rep. **261**, 1 (1995).
[40] X. Ji and C. Chou, Phys. Rev. D **42**, 3637 (1990); R. L. Jaffe and X. Ji, *ibid.* **43**, 724 (1991).
[41] R. L. Jaffe and X. Ji, Phys. Rev. Lett. **67**, 552 (1991).
[42] H. Reinhardt, Phys. Lett. B **244**, 316 (1990); R. Alkofer and H. Reinhardt, *Chiral Quark Dynamics*, Springer Monographs 1995 Vol. 33 (Springer, Berlin, 1995).

[43] D. Ebert and H. Reinhardt, Nucl. Phys. **B271**, 188 (1986).
[44] J. Schwinger, Phys. Rev. **82**, 664 (1951).
[45] C. Christov *et al.*, Prog. Part. Nucl. Phys. **37**, 91 (1996).
[46] R. L. Jaffe, ''*Spin, Twist and Hadron Structure . . .* '' MIT-CTP Report 1996, hep-ph/9602236 (unpublished).
[47] J. D. Bjorken, Phys. Rev. **148**, 1476 (1966).
[48] H. Burkhardt and W. N. Cottingham, Ann. Phys. (N.Y.) **56**, 453 (1970).
[49] H. Weigel, L. Gamberg, and H. Reinhardt, Mod. Phys. Lett. A **11**, 3021 (1996); ''Nucleon Structure Functions from a Chiral Soliton,'' Report No. hep-ph/9604295 [Phys. Lett. B (to be published)].
[50] R. L. Jaffe, Phys. Rev. D **9**, 1444 (1974).
[51] J. Lichtenstadt and H. J. Lipkin, Phys. Lett. B **353**, 119 (1995).
[52] A. V. Efremov, O. V. Teryaev, and E. Leader, Phys. Rev. D **55**, 4307 (1997).
[53] M. Wakamatsu and T. Watabe, Phys. Lett. B **312**, 184 (1993); A. Blotz, M. Prasałowicz, and K. Goeke, *ibid.* **317**, 195 (1993); A. Hosaka and H. Toki, *ibid.* **322**, 1 (1993); C. V. Christov, K. Goeke, P. Pobilista, V. Petrov, M. Wakamatsu, and T. Watabe, *ibid.* **325**, 467 (1994).
[54] R. Alkofer and H. Weigel, Phys. Lett. B **319**, 1 (1993).
[55] J. Schechter and H. Weigel, Phys. Rev. D **51**, 6296 (1995).
[56] R. E. Peierls and J. Yoccoz, Proc. Phys. Soc. London, Sec. A **70**, 381 (1957).
[57] A. J. Signal, Nucl. Phys. **A508**, 493c (1990).
[58] A. Ardekani and A. J. Signal, Phys. Lett. B **311**, 281 (1993).
[59] J. Kodaria *et al.*, Phys. Rev. D **20**, 627 (1979); Nucl. Phys. **B159**, 99 (1979).
[60] E. V. Shuryak and A. I. Vainshtein, Nucl. Phys. **B201**, 141 (1982).
[61] S. Wandzura, and F. Wilczek, Phys. Lett. B **172**, 195 (1987).
[62] F. M. Steffens and A. W. Thomas, Prog. Theor. Phys. Suppl. **120**, 145 (1995).
[63] H. Yabu and K. Ando, Nucl. Phys. **B301**, 601 (1988).
[64] H. Weigel, R. Alkofer, and H. Reinhardt, Nucl. Phys. **B397**, 638 (1992).
[65] S. Kahana and G. Ripka, Nucl. Phys. **A429**, 445 (1984).
[66] R. Alkofer and H. Weigel, Comput. Phys. Commun. **82**, 30 (1994).
[67] D. Diakonov *et al.*, Nucl. Phys. **B480**, 341 (1996).